

Reactivity of phosphido-bridged diplatinum complexes towards electrophiles: synthesis of new hydrides and related Pt₂Cu and Pt₂Ag clusters †

Christine Archambault,^a Robert Bender,^{*a} Pierre Braunstein^{*a} and Yves Dusausoy^b

^a Laboratoire de Chimie de Coordination (UMR 7513 CNRS), Institut Le Bel, Université Louis Pasteur, 4 rue Blaise Pascal, F-67070 Strasbourg-Cédex, France. E-mail: braunst@chimie.u-strasbg.fr; Fax: + 33 390 241 322

^b Laboratoire de Cristallographie et Modélisation des Matériaux Minéraux et Biologiques, UPRESA 7036, Université Henri Poincaré, Nancy I, Faculté des Sciences, Boîte postale 239, F-54206 Vandoeuvre-les-Nancy, France

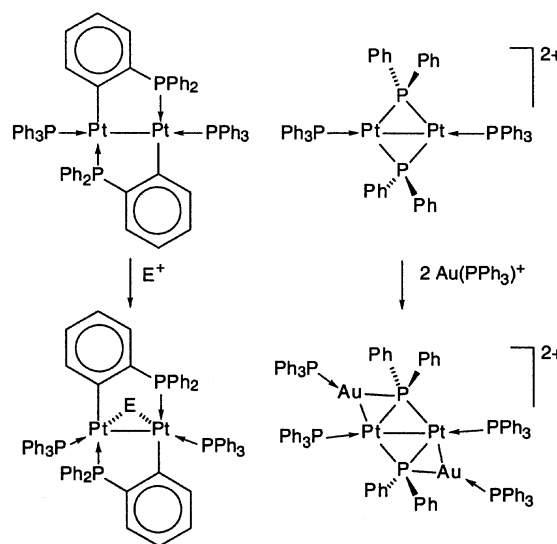
Received 1st July 2002, Accepted 19th September 2002

First published as an Advance Article on the web 22nd October 2002

The doubly-bridged, dinuclear complex [Pt₂(μ-PPh₂)(μ-*o*-C₆H₄PPh₂)(PPh₃)₂] (**1**) reacts with electrophiles such as H⁺ or [M(PPh₃)]⁺ (M = Cu, Ag, Au) first at the metal–metal bond. This is supported by an X-ray diffraction study of [Pt₂{μ-Cu(PPh₃)}(μ-PPh₂)(μ-*o*-C₆H₄PPh₂)(PPh₃)₂]PF₆ (**2**) which reveals a Pt₂Cu triangular metal core and, unexpectedly, a bonding interaction between the Cu atom and the C_{ipso} of the orthometalated phenyl. This confers a tetrahedral-like geometry to the Cu atom. In the neutral complex [Pt₂{μ-AgOC(O)CF₃}(μ-PPh₂)(μ-*o*-C₆H₄PPh₂)(PPh₃)₂] (**3**), the silver atom is coordinated by the terminally bound trifluorocarboxylate anion. Reactions of **1** in a polar solvent with 2 equiv. of acid HA, where A is a weakly nucleophilic anion, afforded the dicationic solvento adducts [Pt₂(μ-H)(μ-PPh₂)(Solv)(PPh₃)₃]A₂ (**5a**, Solv = THF, A = PF₆⁻; **5b**, Solv = CH₂Cl₂, A = BF₄⁻; **5c**, Solv = acetone, A = BF₄⁻) which result from rupture of the Pt–C σ bond and transformation of the cyclometalated bridging ligand into PPh₃. The coordinated solvent molecule is readily displaced by nucleophiles such as PO₂F₂⁻, CF₃SO₃⁻, Cl⁻ or Br⁻, thus forming monocationic complexes, **6–9**, respectively. An X-ray diffraction study on [Pt₂(μ-H)(μ-PPh₂)(OPOF₂)(PPh₃)₃](PF₆)·0.5CH₂Cl₂ (**6**·0.5CH₂Cl₂) establishes that the OPOF₂ group is linked by one O atom to platinum, to our knowledge an unprecedented feature.

Introduction

Diplatinum complexes have been known for several decades and owing to their regularly growing number, they now form a very rich class of compounds with interesting chemistry.¹ Amongst them, the hydrido complexes constitute a large family, with diversified structural and spectroscopic features.^{2–4} The Pt atoms are often linked through metal–metal bonding and/or hydrido bridges. A bridging hydride may also be associated with another, chemically different bridging unit. Although phosphido bridges have often been used to ensure the cohesion of the metallic framework, diplatinum complexes combining phosphido and hydrido bridges are still rather rare,^{3–10} and their synthesis often relies on serendipity.^{7,8} In addition to their own fundamental interest owing to diverse structural and spectroscopic features, platinum complexes are also known for their catalytic properties (*e.g.* in hydrogenation, hydroformylation and hydrosilylation), but only few such studies have been reported with diplatinum complexes.^{11,12} Our interest for the reactivity of diplatinum complexes such as [Pt₂(μ-PPh₂)(μ-*o*-C₆H₄PPh₂)(PPh₃)₂] (**1**), which contains two different, three electron donor bridging groups, a diphenylphosphido ligand and an orthometalated triphenylphosphine, originates from the question of their potential chemoselective reactivity since various sites are available to electrophiles in such molecules.¹³ Whereas [Pt₂(μ-*o*-C₆H₄PPh₂)(PPh₃)₂] reacts with electrophiles at the metal–metal bond,^{14,15} [Pt₂(μ-PPh₂)(PPh₃)₂] adds two equivalents of [Au(PPh₃)]⁺ to give a Pt₂Au₂ cluster resulting



Scheme 1 Addition products of electrophilic reagents E⁺ and Au(PPh₃)⁺ to dinuclear Pt(I)–Pt(I) complexes, as a function of the bridging ligands.

from formal addition of the electrophile to the Pt–(μ-P) bond (Scheme 1)¹⁶ and its dipalladium analogue was shown later to add a proton to a Pd–(μ-P) bond.^{17,18} It therefore appeared particularly interesting to investigate and compare the reactivity of the “mixed-bridged” complex **1** towards electrophilic metal reagents with that of these dinuclear complexes [Pt₂(μ-PPh₂)₂(PPh₃)₂] and [Pt₂(μ-*o*-C₆H₄PPh₂)₂(PPh₃)₂] (Scheme 1).

† Dedicated to Prof. D. Fenske on the occasion of his 60th birthday, with our most sincere congratulations and best wishes.

Previous studies on phosphido-bridged Pt–W complexes have indicated that electrophiles react at the metal–metal bond.^{19,20} We have already evidenced the electron-rich character of the dinuclear complex **1** which contains 16e metal centres and good electron donor ligands.¹³ In this paper, we report the synthesis of a novel, neutral Pt₂Ag complex obtained by reaction of **1** with [AgOC(O)CF₃], the crystal structure of [Pt₂{μ-Cu(PPh₃)}(μ-*o*-C₆H₄PPh₂)(μ-PPh₂)(PPh₃)₂]PF₆ (**2**) which displays an unusual 3c–2e Pt–Cu system, and the reactivity of complex **1** with acids having a poorly coordinating conjugated base, which afforded new cationic hydrido complexes.

Results

Reactions of [Pt₂(μ-PPh₂)(μ-*o*-C₆H₄PPh₂)(PPh₃)₂] (**1**) with electrophilic metal reagents and X-ray structure of [Pt₂{μ-Cu(PPh₃)}(μ-PPh₂)(μ-*o*-C₆H₄PPh₂)(PPh₃)₂]PF₆ (**2**)

We have previously shown that complex **1** reacts with the electrophiles [M(PPh₃)]⁺ (M = Cu, Ag, Au) to afford cationic clusters of general formula [Pt₂{μ-M(PPh₃)}(μ-PPh₂)(μ-*o*-C₆H₄PPh₂)(PPh₃)₂]⁺.¹³ On the basis of their spectroscopic properties, we concluded that the M(PPh₃) fragment bridges the Pt–Pt bond, thus indicating that the basicity of the metal–metal bond in **1** is sufficient to lead to thermodynamically stable addition products. Crystals of **2** suitable for X-ray diffraction could now be obtained, which revealed interesting features (Scheme 2, Fig. 1 and Table 1).

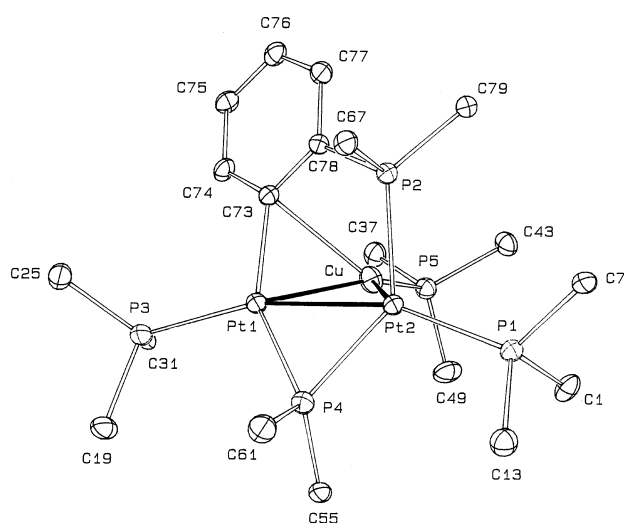


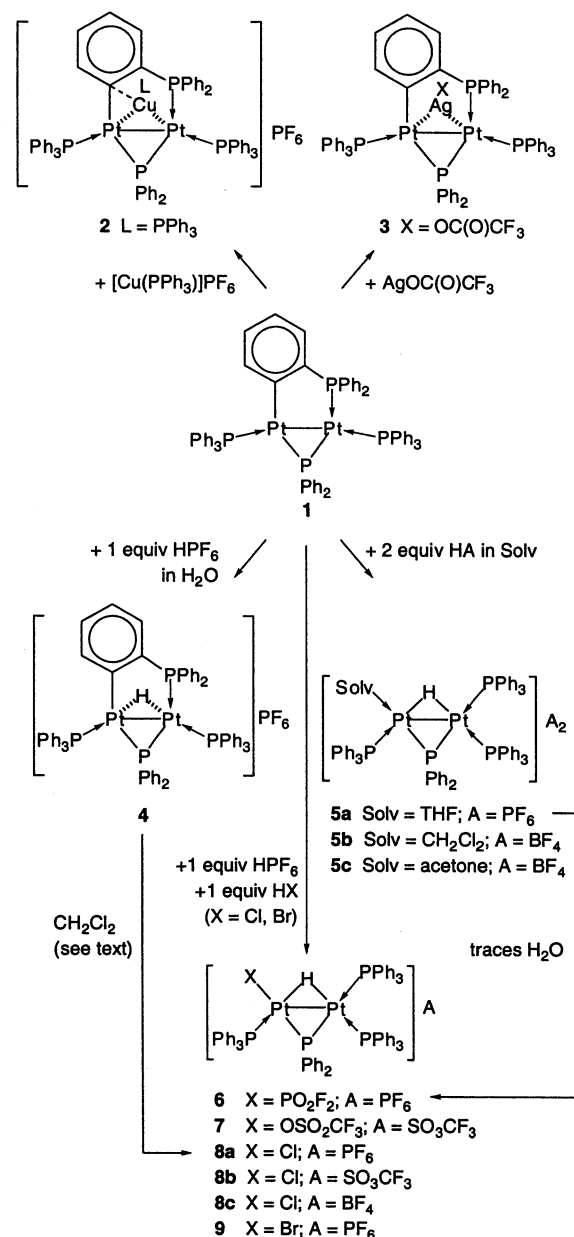
Fig. 1 View of the crystal structure of [Pt₂{μ-Cu(PPh₃)}(μ-PPh₂)(μ-*o*-C₆H₄PPh₂)(PPh₃)₂]PF₆ (**2**) with the atom numbering scheme. Note that the numbering of P(1) and P(3) is interchanged with respect to the labels used for the NMR study of the other compounds and for the structure of 6·0.5CH₂Cl₂ (Fig. 3).

This crystal structure confirms that the Cu atom is linked to both Pt atoms, in a slightly asymmetric fashion [Cu–Pt(1) = 2.536(3) Å and Cu–Pt(2) = 2.595(3) Å] but also reveals an additional, weak interaction between the Cu atom and the p_z orbital of the metalated sp² carbon C(73) [Cu–C(73) = 2.52(1) Å]. The longer Cu–C(78) distance of 2.87(1) Å is not consistent with a description of this interaction as involving the C(73)–C(78) double bond. The Pt₂Cu plane makes a dihedral angle of 64.0(1)° with the mean plane of the core atoms Pt(1), P(4), Pt(2), P(2), C(78) and C(73). The coordination of the Cu(PPh₃) fragment to **1** does not significantly affect the geometry and bonding parameters of the latter moiety; in particular the Pt–Pt distances in complexes **1** and **2** are similar.¹³ The largest variations observed on going from **1** to **2** are in the P(2)–C(78)–C(73) orthometalated bridge, with a slight closing of the C(73)–C(78)–P(2) angle from 124(2) to 118.4(7)°, and an opening of

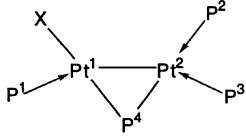
Table 1 Selected bond distances (Å) and angles (°) for [Pt₂{μ-Cu(PPh₃)}(μ-PPh₂)(μ-*o*-C₆H₄PPh₂)(PPh₃)₂]PF₆ (**2**)^a

Pt(1)–Pt(2)	2.657(1)	Pt(2)–P(1)	2.302(5)
Pt(1)–Cu	2.536(3)	Pt(2)–P(2)	2.283(5)
Pt(2)–Cu	2.595(3)	Pt(2)–P(4)	2.292(5)
Pt(1)–P(3)	2.278(6)	Cu–P(5)	2.180(6)
Pt(1)–P(4)	2.248(5)	Cu–C(73)	2.52(1)
Pt(1)–C(73)	2.11(2)	Cu–C(78)	2.87(1)
		C(73)–C(78)	1.39(1)
Cu–Pt(1)–P(4)	96.2(1)	P(2)–C(78)–C(73)	118.4(7)
Pt(2)–Pt(1)–P(4)	55.0(1)	Pt(1)–Pt(2)–Cu	57.7(1)
Pt(2)–Pt(1)–P(3)	162.8(1)	Pt(1)–Pt(2)–P(4)	53.4(1)
Pt(2)–Pt(1)–Cu	59.9(1)	Cu–Pt(2)–P(4)	93.5(2)
P(3)–Pt(1)–C(73)	102.0(3)	Pt(1)–Pt(2)–P(2)	85.3(1)
Cu–Pt(1)–C(73)	64.9(3)	Cu–Pt(2)–P(2)	76.5(2)
C(73)–Pt(1)–Pt(2)	95.2(3)	Pt(1)–Pt(2)–P(1)	160.9(1)
Pt(1)–Cu–Pt(2)	62.4(1)	Cu–Pt(2)–P(1)	125.8(1)
P(5)–Cu–Pt(1)	151.5(2)	P(1)–Pt(2)–P(2)	113.8(2)
P(5)–Cu–Pt(2)	139.0(1)	Pt(2)–P(4)–Pt(1)	71.6(2)
Pt(1)–C(73)–C(78)	120.9(7)	Pt(2)–P(2)–C(78)	113.8(4)

^a For the numbering of the atoms, see Fig. 1. The P(1) and P(3) labels are interchanged in the NMR section.



Scheme 2

Table 2 Selected ^1H and $^{31}\text{P}\{^1\text{H}\}$ NMR data for complexes **1** and **3–9** (δ in ppm and J in Hz)


	1	3	4	5a	5b	5c	6	7	8	9
$\delta(^1\text{H})$	—	—	−5.10	—	−5.44	—	−5.08	—	−4.68	−4.58
$^1J(\text{H–Pt})$	—	—	383, 521	—	418, 489	—	385, 517	—	367, 524	372, 519
$^2J(\text{H–P})$	—	—	80, 68, 14.5, 14.5	—	75, 67, 14, 14	—	80, 70, 15	—	81, 70, 15.5, 13.5	80, 70, 15, 13
$\delta(\text{P}^1)$	28.4	29.1	23.3	14.8	14.7	15.3	15.6	14.9	14.6	14.3
$\delta(\text{P}^2)$	9.1	16.0	28.4	10.3	9.0	9.0	11.3	11.5	10.5	10.8
$\delta(\text{P}^3)$	31.3	31.0	30.4	22.7	23.1	23.4	23.3	23.3	21.5	20.7
$\delta(\text{P}^4)$	164.6	182.2	167.8	112.1	113.8	114.3	112.5	114	132.2	139.6
$^1J(\text{P}^1\text{–Pt}^1)$	3607	3799	3770	3902	3899	3935	3890	3887	3895	3893
$^1J(\text{P}^2\text{–Pt}^2)$	3210	2809	3046	2422	2450	2472	2417	2453	2392	2407
$^1J(\text{P}^3\text{–Pt}^2)$	3343	3575	4575	4384	4380	4375	4388	4385	4340	4306
$^1J(\text{P}^4\text{–Pt}^1)$	2116	2078	3505	1855	1878	1885	1847	1859	1872	1902
$^1J(\text{P}^4\text{–Pt}^2)$	2645	2435	4778	3336	3207	3192	3315	3388	2942	2904
$^2J(\text{P}^1\text{–Pt}^2)$	215	214	40	249	249	—	223	—	213	211
$^2J(\text{P}^2\text{–Pt}^1)$	73	55.5	98	36	66	—	73	63	64	63
$^2J(\text{P}^3\text{–Pt}^1)$	526	322	94	266	238	221	255	255	300	298
$^3J(\text{P}^1\text{–P}^2)$	6	—	—	20	20	—	21	19	20	20
$^3J(\text{P}^1\text{–P}^3)$	151	140	109	50	49	45	—	47	57	58
$^2J(\text{P}^1\text{–P}^4)$	30	17	60	8	—	—	—	—	10	8
$^2J(\text{P}^2\text{–P}^3)$	9	—	—	—	—	—	—	—	—	—
$^2J(\text{P}^2\text{–P}^4)$	213	220	279	277	282	283	277	279	264	264
$^2J(\text{P}^3\text{–P}^4)$	< 5	—	58	—	—	—	—	—	—	—

the P(3)–Pt(1)–C(73) angle from 98.5(5) to 102.0(3) $^\circ$ and of the Pt(1)–C(73)–C(78) angle from 114(1) to 120.9(7) $^\circ$. These deformations are probably induced by the 2e–3c Pt–C(73)–Cu interaction. Crystal structures of complexes containing a Pt–Cu bond are rather rare,^{21a} and only three of them contain a Pt–Cu–phosphine sequence.^{22–24} The Pt–Cu distances in **2** are close to those observed in [CuPt₃(μ -CO)₃(PPh₃)₃]BF₄, where the Cu(PPh₃) group caps a triangle of Pt atoms.²² The Cu–P distance in **2** is shorter than those observed in other complexes containing the Cu–PPh₃ moiety.^{22,23,25}

Complex **1** reacted with 1 equiv. [AgOC(O)CF₃] in toluene at room temperature to afford the neutral, heterotrimeric cluster [Pt₂{ μ -AgOC(O)CF₃}(μ -PPh₂)(μ -*o*-C₆H₄PPh₂)(PPh₃)₂] (**3**). This compound is soluble in THF, CH₂Cl₂ or in toluene where it slowly decomposes at room temperature with formation of metallic silver, in the daylight or in the dark. The IR spectrum of **3** showed intense absorption bands at 1667, 1200 and 1135 cm^{−1} due to the trifluoroacetato ligand and a medium band at 724 cm^{−1} characteristic of the orthometalation.¹³ The mass spectrum of **3** did not contain the peak corresponding to M⁺ at *m/z* = 1576.9, but peaks at 1469.1 and 1361.2 due to the fragments [M–CF₃CO₂]⁺ and [M–AgOC(O)CF₃]⁺ (**1**⁺), respectively.

The $^{31}\text{P}\{^1\text{H}\}$ NMR spectrum of **3** resembles that of **1** with resonances for four chemically and magnetically different ^{31}P nuclei, flanked by satellites due to 1 or $^2J(\text{P–Pt})$ couplings (Table 2). The chemical shifts and coupling constants 2 or $^3J(\text{P–P})$ and 1 or $^2J(\text{P–Pt})$ are comparable to those for the Pt₂P₄ core of the related cationic cluster [Pt₂{ μ -Ag(PPh₃)₂}(μ -PPh₂)(μ -*o*-C₆H₄PPh₂)(PPh₃)₂]⁺.¹³ The P(2) and P(4) nuclei of **3** are only slightly deshielded when compared with those in complex **1**. Their 2 or $^3J(\text{P–P})$ values are almost identical and the 1 or $^2J(\text{P–Pt})$ vary only slightly, remaining in the usual range.^{7,8} The $^{31}\text{P}\{^1\text{H}\}$ NMR spectrum of **3** has been satisfactorily simulated using the gNMR software for three of the four isotopomers, those with the spin systems ABEM (M = μ -P, abundance 43.82%, no ¹⁹⁵Pt), ABEMX (X = ¹⁹⁵Pt(1), 22.38%) and ABEMY (Y = ¹⁹⁵Pt(2), 22.38%). The spectrum of the isotopomer with the spin system ABEMXY (X, Y = ¹⁹⁵Pt, 11.42%) has not been simulated because the corresponding signals were too weak to be clearly identified in the experimental spectrum. The spectral

simulations afforded chemical shifts and coupling constants very similar to the experimental values and they confirmed the analysis of the spectrum. Therefore, the experimental values for **3** may be used with confidence for the description of this spectrum. For consistency, only the experimental values of the other compounds are reported (Table 2).

The most deshielded $^{31}\text{P}\{^1\text{H}\}$ NMR resonance (δ 182.2 ppm) is attributed to the bridging P(4) atom, its chemical shift indicating the presence of a Pt–Pt bond.²⁶ The other three signals belong to the terminal and orthometalated phosphines. The large value of the P–P coupling constants correspond to nuclei in mutual *trans* positions: P(2) and P(4) with $^2J(\text{P}(2)\text{–P}(4))$ = 220 Hz and P(1) and P(3) with $^3J(\text{P}(1)\text{–P}(3))$ = 140 Hz. The small values of the other P–P couplings or their absence are due to the relative *cis* positions of P(1) and P(4) with $^2J(\text{P}(1)\text{–P}(4))$ = 17 Hz and of P(3) and P(2) and P(4), respectively. No $^2J(\text{Ag–P})$ coupling constant could be observed in the spectrum, in contrast to the case of the complex cation [Pt₂{ μ -Ag-(PPh₃)₂}(μ -PPh₂)(μ -*o*-C₆H₄PPh₂)(PPh₃)₂]⁺.¹³ Nevertheless, on the basis of the spectroscopic data available, we assign to cluster **3** a structure comparable to that of **2**, *i.e.* with a planar Pt₂P₄ core, as in **1**, and the AgOC(O)CF₃ group bridging the Pt–Pt bond. This group has previously been found to coordinate to the triplatinum core of [Pt₃(μ -PPh₂)₃Ph(PPh₃)₃] to form a tetrahedral Pt₃Ag cluster in which the CF₃CO₂ ligand is coordinated to Ag by only one oxygen atom.²⁷ Since the trifluoroacetate ligand leads in the IR spectrum to the same three absorptions in both clusters, we propose a similar coordination mode for this ligand on the Ag atom in **3**.

Reactions of [Pt₂(μ -PPh₂)(μ -*o*-C₆H₄PPh₂)(PPh₃)₂] (**1**) with acids

The reaction of a THF solution of the diplatinum complex **1** with 1 equiv. HPF₆ diluted in H₂O afforded complex **4** whereas reaction of **1** in a polar solvent with 2 equiv. of acid HA, where A is a weakly nucleophilic conjugated base, afforded the dicationic solvento adducts [Pt₂(μ -H)(μ -PPh₂)(Solv)(PPh₃)₃]A₂ (**5a**, Solv = THF, A = PF₆[−]; **5b**, Solv = CH₂Cl₂, A = BF₄[−]; **5c**, Solv = acetone, A = BF₄[−]) (Scheme 2). Complex **5a** is insoluble in THF and upon dissolution in CH₂Cl₂, its coordinated THF

molecule probably exchanges with CH_2Cl_2 , as indicated by the similarity of its ^{31}P NMR spectrum with that of **5b**. The slight differences observed may be due to incomplete displacement of THF, which is a better donor ligand than CH_2Cl_2 ,^{28a} although in our case the latter is present in considerable excess. Furthermore, **5a** is difficult to dry and the remaining water resulted in rapid hydrolysis, in CH_2Cl_2 solution, of one of the PF_6 anions, affording compound **6**, which contains a PO_2F_2 anion as ligand in place of the solvent molecule. A related complex, $[\text{Pt}_2(\mu\text{-H})(\mu\text{-PPh}_2)(\text{OSO}_2\text{CF}_3)(\text{PPh}_3)_3](\text{SO}_3\text{CF}_3)$ (**7**), was obtained by reaction of **1** with 2 equiv. of $\text{CF}_3\text{SO}_3\text{H}$. The ^{31}P NMR spectra of **6** and **7** are very similar (Table 2). Dichloromethane solutions of **5b** contained small quantities of the BF_4 salt of the monocationic chloro complex present in **8**, as seen by $^{31}\text{P}\{^1\text{H}\}$ NMR (Scheme 2). The same cation was formed quantitatively by reaction of **1** with a mixture of 1 equiv. HCl and 1 equiv. HPF_6 or $\text{CF}_3\text{SO}_3\text{H}$. Its bromo analogue **9** was obtained by reaction of **1** with a mixture of 1 equiv. HBr and 1 equiv. HPF_6 (Scheme 2). Unexpectedly, crystals of **8c** were obtained upon crystallisation from $\text{CH}_2\text{Cl}_2/\text{Et}_2\text{O}$ of the BF_4 analogue of **4**. Although the poor quality of the crystals prevented complete structural resolution, both the core structure of the dinuclear cation contained in **8** and the presence of the chloro ligand, which must originate from the solvent (or from HCl contamination), have been confirmed by a preliminary X-ray diffraction study.²⁹

The new complexes **4–9** present in their IR spectra absorption bands characteristic of their anions: $\nu(\text{PF}_6^-) = 836\text{--}839\text{ cm}^{-1}$, $\nu(\text{BF}_4^-) = 1055\text{ cm}^{-1}$, $\nu(\text{CF}_3\text{SO}_3^-) = 1260$ and $1125 (\text{SO}_3)$ and 1220 and 1140 cm^{-1} (CF_3).^{28b} In addition, PF_6^- shows the usual septet in the $^{31}\text{P}\{^1\text{H}\}$ NMR spectrum at $\delta -143$, with $^1J(\text{P-F}) = 711\text{ Hz}$.³⁰ Only **4** shows the characteristic orthometalation absorption at 724 cm^{-1} ,¹³ thus indicating that after protonation of **1**, the orthometalation P–C bond was retained in **4**, but cleaved in **5–9**. The free coordination site thus liberated was occupied by a molecule of solvent, THF, CH_2Cl_2 or acetone or by the anions OPOF_2 , OSO_2CF_3 , Cl or Br . The presence of THF was evidenced by ^1H NMR spectroscopy of a solution of **5a** in CH_2Cl_2 , with two triplets of equal intensity at $\delta 1.85$ and 3.75 , respectively, due to the THF liberated upon dissolution. The acetone ligand of **5c** accounts for an IR $\nu(\text{C=O})$ absorption band at 1642 cm^{-1} . The PO_2F_2 ligand in **6** leads in the IR spectrum to $\nu(\text{PO})$ and $\nu(\text{PF})$ bands at 1312 (vs) and 838 (vs) cm^{-1} , respectively,^{30–32} and in the $^{31}\text{P}\{^1\text{H}\}$ NMR spectrum to a broad triplet at $\delta -16.7$ ($^1J(\text{PF}) = 967\text{ Hz}$),³³ which suggests small, unresolved coupling constants with Pt and other P nuclei.

The similarity of the $^{31}\text{P}\{^1\text{H}\}$ NMR spectra of **1** with those of complexes **4–9** suggests analogous molecular structures for these complexes. These spectra, as well as the ^1H NMR spectra, could be analyzed using the first order approximation since spectral simulations using gNMR gave very similar values to the experimental ones, for complex **4**, as well as for **3**. Therefore only the absolute values of the coupling constants are reported in Table 2. Like **1**, the new complexes display $^{31}\text{P}\{^1\text{H}\}$ NMR spectral patterns corresponding to four chemically and magnetically different ^{31}P nuclei, all of them being flanked by satellites due to 1 or $^2J(\text{P-Pt})$ couplings. In all these complexes, P(4) resonates at low field, indicating a phosphido group bridging a metal–metal bond, while the other resonances are in the usual range for terminal phosphines. The large value of *ca.* 270 Hz for $^2J[\text{P}(2)\text{--P}(4)]$ in complexes **4–9** indicates the mutual *trans* position of these nuclei.

On going from **1** to **4**, the values of $^1J[\text{Pt}(2)\text{--P}(3)]$ and of both $^1J[\text{Pt}\text{--P}(4)]$ couplings increase significantly, with the latter being among the largest values found for $^1J(\text{Pt}\text{--P})$ couplings involving a $\mu\text{-PPh}_2$ group. In contrast, a comparison of **4** with **5–9** shows a decrease of $^1J[\text{Pt}\text{--P}(2)]$ and $^1J[\text{Pt}\text{--P}(4)]$, while $^1J[\text{Pt}\text{--P}(1$ or $3)]$ remain comparable. The ^1H NMR spectra of the new complexes **4–9** contain a dddd pattern around -5 ppm, with two sets of satellites due to two different $^1J(\text{H}\text{--Pt})$ couplings, in the range 367–418 and 489–524 Hz, respectively (Fig. 2). The multi-

licity of this signal arises from four $^2J(\text{P}\text{--H})$ coupling constants, two of them of *ca.* 14 Hz for two ^{31}P nuclei in *cis* position with respect to the proton and the other two of *ca.* 70 and 80 Hz due to two ^{31}P nuclei in *trans* positions. These data are indicative of the bridging position of the proton on the Pt–Pt bond, as found for the isolobal $[\text{Cu}(\text{PPh}_3)]^+$ group in cluster **2**.

Molecular structure of $[\text{Pt}_2(\mu\text{-H})(\mu\text{-PPh}_2)(\text{OPOF}_2)(\text{PPh}_3)_3](\text{PF}_6)\cdot 0.5\text{CH}_2\text{Cl}_2$ (**6**· $0.5\text{CH}_2\text{Cl}_2$)

The molecular structure of **6**· $0.5\text{CH}_2\text{Cl}_2$ has been determined by X-ray diffraction on crystals obtained from a mixture $\text{CH}_2\text{Cl}_2/\text{diethyl ether}$. A view of the structure is shown in Fig. 3 and selected bond distances and angles are reported in Table 3. This structure is based on two Pt atoms linked by a metal–metal bond [$\text{Pt}(1)\text{--Pt}(2) = 2.8711(4)\text{ \AA}$] and an asymmetric PPh_2 bridge [$\text{Pt}(1)\text{--P}(4) = 2.206(2)\text{ \AA}$, $\text{Pt}(2)\text{--P}(4) = 2.296(2)\text{ \AA}$]. These values are in the range found in structurally related molecules.^{7,8}

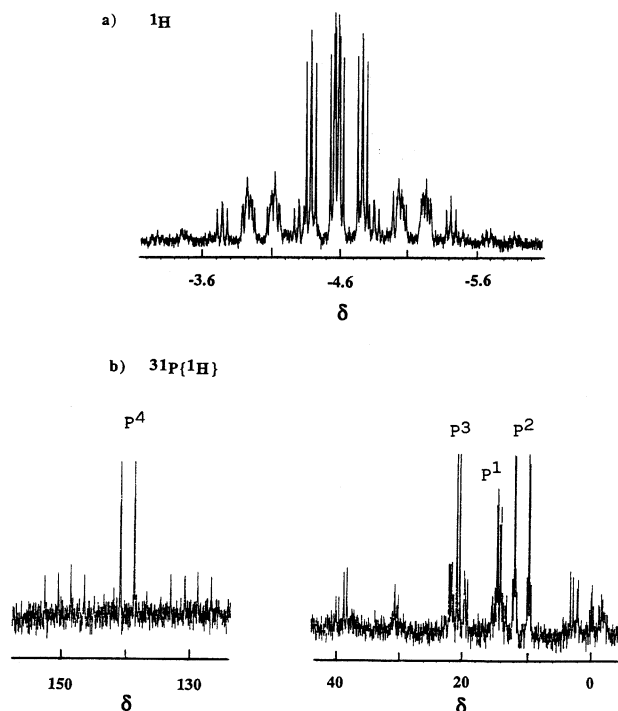


Fig. 2 (a) ^1H and (b) $^{31}\text{P}\{^1\text{H}\}$ NMR spectra of $[\text{Pt}_2(\mu\text{-H})(\mu\text{-PPh}_2)\text{Br}(\text{PPh}_3)_3](\text{PF}_6)$ (**9**) in CD_2Cl_2 .

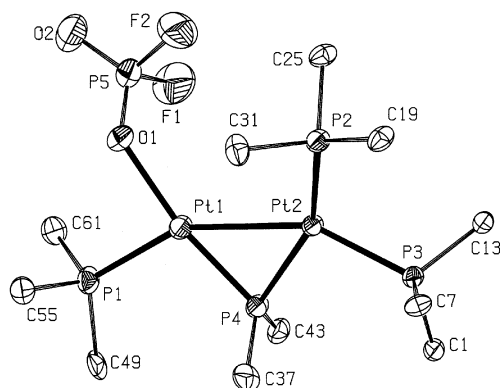


Fig. 3 View of the crystal structure of $[\text{Pt}_2(\mu\text{-H})(\mu\text{-PPh}_2)(\text{OPOF}_2)(\text{PPh}_3)_3](\text{PF}_6)$ in **6**· $0.5\text{CH}_2\text{Cl}_2$ with the atom numbering scheme. For clarity, only the *ipso* phenyl carbons are represented and the hydride ligand bridging the $\text{Pt}(1)\text{--Pt}(2)$ bond is not shown. The projection view is not in the plane $\text{Pt}(1)\text{--Pt}(2)\text{--P}(4)$.

Table 3 Selected bond distances (Å) and angles (°) for [Pt₂(μ-H)(μ-PPh₂)(OPOF₂(PPh₃)₃)(PF₆)·0.5CH₂Cl₂ (**6**·0.5CH₂Cl₂)

Pt(1)–Pt(2)	2.8711(4)	Pt(2)–P(4)	2.296(2)
Pt(1)–P(1)	2.282(2)	P(5)–O(1)	1.494(5)
Pt(1)–O(1)	2.156(4)	P(5)–O(2)	1.432(6)
Pt(1)–P(4)	2.206(2)	P(5)–F(1)	1.546(5)
Pt(2)–P(2)	2.355(2)	P(5)–F(2)	1.547(6)
Pt(2)–P(3)	2.291(2)		
P(1)–Pt(1)–Pt(2)	153.13(5)	P(3)–Pt(2)–P(4)	101.39(6)
P(1)–Pt(1)–P(4)	102.42(6)	Pt(1)–Pt(2)–P(4)	49.00(4)
P(1)–Pt(1)–O(1)	87.2(1)	Pt(1)–P(4)–Pt(2)	79.24(5)
O(1)–Pt(1)–Pt(2)	119.2(1)	O(1)–P(5)–O(2)	121.3(3)
O(1)–Pt(1)–P(4)	169.7(1)	O(1)–P(5)–F(1)	109.0(3)
Pt(2)–Pt(1)–P(4)	51.76(4)	O(1)–P(5)–F(2)	106.9(3)
P(2)–Pt(2)–Pt(1)	108.46(4)	F(1)–P(5)–O(2)	110.5(3)
P(2)–Pt(2)–P(4)	152.41(6)	F(2)–P(5)–O(2)	108.2(4)
P(2)–Pt(2)–P(3)	99.42(6)	F(1)–P(5)–F(2)	98.6(4)
Pt(1)–Pt(2)–P(3)	150.47(4)	P(5)–O(1)–Pt(1)	130.3(3)

Two terminal phosphines P(1) and P(3) lie respectively in *trans* position to the Pt–Pt bond, and the coordination spheres of the metal atoms are completed by an OPOF₂ ligand for Pt(1) and a third phosphine P(2) for Pt(2). The latter ligands are both in *transoid* position with respect to the μ-PPh₂ group. The OPOF₂ group is linked by one O atom to Pt(1), to our knowledge an unprecedented feature, although the distances and angles within this ligand are in good agreement with the rare examples found in the literature for a monocoordinated difluorophosphate on other metals.^{30,33–36} The core atoms of **6**, Pt(1), Pt(2), P(1), P(3), P(4) and O(1) are almost coplanar; the P(2) atom lies at 1.017 Å from their mean plane. This confirms the results of the ³¹P{¹H} NMR study. A PF₆[−] anion and half a molecule of CH₂Cl₂ of crystallisation are associated with each dinuclear cation. The bridging proton evidenced by ¹H NMR spectroscopy could not be located in the X-ray study, but the long Pt(1)–Pt(2) distance is indicative of such a bridge.^{7,8}

Discussion

The Pt–Pt bond of complex **1** is sufficiently electron-rich to coordinate a proton or the isolobal electrophilic groups [M(PPh₃)₃]⁺ (M = Cu, Ag, Au). This indicates for **1** a reactivity towards electrophiles closer to that of [Pt₂(μ-*o*-C₆H₄PPh₂)₂(PPh₃)₂]^{14,15} than of [Pt₂(μ-PPh₂)₂(PPh₃)₂].¹⁶ The molecular structure of the Pt₂Cu cluster **2** shows that the core structure of its precursor **1** is not significantly altered and the Pt–Pt bond distance is similar in both complexes, suggesting that the interaction of the [Cu(PPh₃)₃]⁺ group with **1** is weak. The relatively short Cu–C(73) distance indicates a bonding interaction of the Cu atom with this C_{ipso} of the orthometalated phenyl, which confers a tetrahedral-like geometry to the Cu atom, preferred here over the trigonal one.²³ Although related bonding situations have been observed in homonuclear Pt₃ complexes,³⁷ such situations are relatively rare with copper^{38,39} and **2** appears to be the first example of a 2e–3c bond involving a Pt–C–Cu(PPh₃) moiety. In the Pt₂Ag cluster **3**, the neutral fragment AgOC(O)CF₃ also occupies a bridging position on the Pt–Pt bond of **1**. It is often more difficult or even impossible to obtain stable complexes with group 11 metals other than gold, which is related to the increased lability of the related copper and silver complexes.²¹ Thus for example, the diplatinum complex [Pt₂(μ-PPh₂)₂(PPh₃)₂] formed a stable compound with two Au(PPh₃)⁺ fragments (Scheme 1),¹⁶ while neither [Cu(PPh₃)₃]⁺, [Ag(PPh₃)₃]⁺ nor [AgOC(O)CF₃] gave stable, isolable compounds. Cluster **3** is not as stable as the related cationic cluster [Pt₂{μ-Ag(PPh₃)₃}(μ-PPh₂)(μ-*o*-C₆H₄PPh₂)(PPh₃)₂]⁺, but the stabilisation of Ag(I) by the O atom of CF₃CO₂ permits its isolation and seems to slow down the redox process that leads to the formation of metallic silver.

When an acid with a weakly coordinating conjugated base was reacted with **1**, the proton goes to a bridging position on the Pt–Pt bond of **1**, without rupture of the orthometalated Pt–C bond. Only a second proton induces the breaking of this bond, with formation of a terminal triphenylphosphine ligand and liberation of a vacant coordination site on platinum, which is then occupied by a solvent molecule. The resulting complexes **5** are thus dicationic. When a more nucleophilic reagent X[−] is present in solution (X = PO₂F₂, CF₃SO₃, Cl, Br), it occupies this vacant site to form a new monocationic complex, **6–9**, respectively. Although monocationic diplatinum hydrides have long been known,^{3a} and can adopt various geometries,² examples containing an additional phosphido bridge are rarer,^{3,5–9} and, to our knowledge, no such dicationic species has been previously observed.

The orthometalated Pt–C bond is no longer present in complexes **5–9** and these complexes present a similar set of NMR data, suggesting that their geometry and the localization of the bridging proton are similar, probably in the Pt₂P₄ plane of the cation. A similar disposition is found in [Pt₂Ph(μ-H)(μ-PPh₂)(PPh₃)₃]^{7,8}. Complex **4** shows a set of ³¹P NMR resonances of which some are very different from those of **1** or **5–9**. This could be the consequence of a different geometry for **4**, and particularly a non-planarity of the Pt₂P₄ core. Indeed, the persistence of the orthometalated cycle in **4** certainly hinders the localization of the proton in this plane and as a consequence, P(1) and P(3), which lie in *transoid* positions with respect to the proton and whose ²J(P–Pt) are much lower compared to the other complexes, should be located out of the molecular plane, on the opposite side to the proton (A-frame type structure). The opening of the Pt–C bond in complexes **5–9** allows a rearrangement of the geometry of **4** into a planar one, with the bridging proton located now between the former orthometalated phosphine P(2) and the new incoming ligand (solvent or ligand X).

All complexes **1** and **4–9** possess 30 electrons and display a metal–metal bond, which leads to a 16e environment for each Pt atom. In **1**, both Pt atoms should be formally considered as Pt(I), whereas in complexes **4–9**, they are better considered as Pt(II) centres, as in [Pt₂Ph(μ-H)(μ-PPh₂)(PPh₃)₃]⁺. With this formalism, the incoming proton has been formally reduced into a hydride and both Pt atoms have been oxidized from Pt(I) to Pt(II). The second proton, upon breaking the metal–carbon σ bond of the orthometalated phenyl group, does not change the oxidation state of the Pt atoms in complexes **5–9**.

Experimental

All experiments were performed under an inert atmosphere of deoxygenated and dried nitrogen with the use of the Schlenk techniques. The complexes [Pt₂(μ-*o*-C₆H₄PPh₂)(μ-PPh₂)(PPh₃)₂] and [Pt₂{μ-Cu(PPh₃)₃}(μ-PPh₂)(μ-*o*-C₆H₄PPh₂)(PPh₃)₂](PF₆) were prepared as described in the literature.¹³ Solvents were dried and distilled under nitrogen prior to use. Infrared spectra were measured in KBr pellets on a Nicolet 205 FT-IR spectrometer and NMR spectra on Bruker AM 400 (³¹P at 161.977 MHz) and on a FT-Bruker WP 200 SY instrument (³¹P at 81.02 MHz and ¹H at 200.13 MHz). Phosphorus chemical shifts were externally referenced to 85% H₃PO₄ in H₂O, with downfield chemical shifts reported as positive. Proton chemical shifts were positive downfield relative to external SiMe₄. FAB mass spectra were measured using a VG ZAB-HF mass spectrometer, in a NBA matrix.

Preparations

[Pt₂{μ-AgOC(O)CF₃}(μ-*o*-C₆H₄PPh₂)(μ-PPh₂)(PPh₃)₂] (**3**). Toluene (3 mL) was added to a mixture of solid [Pt₂(μ-PPh₂)(μ-*o*-C₆H₄PPh₂)(PPh₃)₂] **1** (170 mg, 0.125 mmol) and [AgOC(O)CF₃] (29 mg, 0.131 mmol, 5% excess). The mixture was stirred at

room temperature for 5 min and its colour quickly turned brown. Addition of hexane (*ca.* 5 mL) yielded a beige powder of **3** (154 mg, 78%). Anal. calc. for $C_{68}H_{54}AgF_3O_2P_4Pt_2$ ($M_r = 1582.09$): C, 51.62; H, 3.44. Found: C, 52.77; H, 3.75. IR (KBr): 1667(s), 1200(s), 1135(s) cm^{-1} (CF_3CO_2), 724(m) cm^{-1} (ν orthometalation). FABMS (p - $O_2NC_6H_4CH_2OH$, NBA matrix): $m/z = 1469.1$ ($M - CF_3CO_2$) $^+$, 1361.2 ($M - CF_3CO_2Ag$) $^+$. Details of the $^{31}P\{^1H\}$ and 1H NMR studies are summarized in Table 2.

[Pt₂(μ -H)(μ -PPh₂)(μ -*o*-C₆H₄PPh₂)(PPh₃)₂]PF₆ (4**).** HPF₆ (10.5 μ L, 75% in H₂O, 0.1 mmol) was added to a solution of [Pt₂(μ -PPh₂)(μ -*o*-C₆H₄PPh₂)(PPh₃)₂] (**1**) (136.8 mg, 0.1 mmol) in THF (15 mL). The colour of the solution rapidly changed from orange to red and then to pale orange. The mixture was stirred for 5 h at room temperature and the solvent was evaporated to dryness under reduced pressure. The $^{31}P\{^1H\}$ NMR spectrum of the solid residue dissolved in CH₂Cl₂/C₆D₆ showed only one product formed in quantitative yield. Anal. calc. for $C_{66}H_{55}F_6P_5Pt_2$ ($M_r = 1507.182$): C, 52.60; H, 3.68. Found: C 51.21; H, 4.05. IR (KBr): 836(s) (PF₆) cm^{-1} . FABMS (p - $O_2NC_6H_4CH_2OH$) (NBA matrix): $m/z = 1361.0$ (M) $^+$, 1283.9 (M - Ph) $^+$, 1098.9 (M - PPh₃) $^+$, 1021.8 (M - PPh₃ - Ph) $^+$. See NMR details in Table 2.

[Pt₂(μ -H)(μ -PPh₂)(PPh₃)₃(THF)](PF₆)₂ (5a**).** HPF₆ (13 μ L, 75% in H₂O, 0.124 mmol) was added to a solution of **1** (84.5 mg, 0.062 mmol) in THF (15 mL). The colour of the solution rapidly changed from orange to yellow. After stirring at room temperature for 1 h, a white precipitate was formed, filtered, washed with cold THF and dried under reduced pressure. Complex **5a** was isolated in 71% yield. Anal. calc. for $C_{70}H_{64}OF_{12}P_6Pt_2$ ($M_r = 1725.26$): C, 48.73; H, 3.74. Found: C, 48.60; H, 3.58. IR (nujol): 838 (s) (PF₆) cm^{-1} .

[Pt₂(μ -H)(μ -PPh₂)(PPh₃)₃(CH₂Cl₂)](BF₄)₂ (5b**).** HBF₄ (42 μ L, 34% in H₂O, 0.20 mmol) was added to a solution of [Pt₂(μ -PPh₂)(μ -*o*-C₆H₄PPh₂)(PPh₃)₂] **1** (136 mg, 0.10 mmol) in CH₂Cl₂ (50 mL). The colour of the solution rapidly changed from orange to pale yellow. After stirring at room temperature for 4 h, evaporation of the solvent under reduced pressure overnight afforded a yellow precipitate. See NMR details in Table 2.

[Pt₂(μ -H)(μ -PPh₂)(PPh₃)₃{(CH₃)₂CO}](BF₄)₂ (5c**).** The procedure was similar to that for **5b**, except that the reaction was carried out in acetone (50 mL). Recrystallisation from a mixture of acetone and diethyl ether gave colourless **5c** as shown by $^{31}P\{^1H\}$ NMR. IR (KBr): 1644 (m) (ν (C=O) of coordinated acetone), 1054(s) (ν (BF₄)) cm^{-1} . See NMR details in Table 2.

[Pt₂(μ -H)(μ -PPh₂)(OPOF₂)(PPh₃)₃](PF₆) \cdot 0.5CH₂Cl₂ (6**·0.5CH₂Cl₂).** When **5a** was not carefully dried and contained residual water, it transformed in CH₂Cl₂ into [Pt₂(μ -H)(μ -PPh₂)(OPOF₂)(PPh₃)₃]PF₆ **6** in less than 2 h, as seen by 1H and $^{31}P\{^1H\}$ NMR (see details in Table 2). Traces of **8a** are also present. X-ray quality crystals of **6**·0.5CH₂Cl₂ were obtained by addition of diethyl ether to this solution and crystallisation at room temperature. IR (KBr): 1312 (ν (PO)), 837 (ν (PF₆)) cm^{-1} .

[Pt₂(μ -H)(μ -PPh₂)(PPh₃)₃(OSO₂CF₃)](SO₃CF₃) (7**).** Pure CF₃SO₃H (44 μ L, 0.5 mmol) was added to a solution of **1** (136.8 mg, 0.1 mmol) in CH₂Cl₂ (15 mL). The colour of the solution rapidly turned from orange to pale yellow. After stirring for 5 h at room temperature, addition of diethyl ether afforded colourless crystals (110 mg, yield 72%). The purity of the solid was checked by $^{31}P\{^1H\}$ NMR in a CH₂Cl₂-CD₂Cl₂ mixture. See NMR details in Table 2.

Table 4 Crystallographic details for [Pt₂Cu{ μ -*o*-C₆H₄PPh₂}(μ -PPh₂)-(PPh₃)₃][PF₆] (**2**) and [Pt₂(μ -H)(μ -PPh₂)(OPOF₂)(PPh₃)₃][PF₆] \cdot 0.5CH₂Cl₂ (**6**·0.5CH₂Cl₂)

	2	6 ·0.5CH ₂ Cl ₂
Formula	C ₆₄ H ₆₉ CuF ₆ P ₆ Pt ₂	C _{66.5} H ₅₇ ClF ₈ O ₂ P ₆ Pt
<i>M</i>	1832.04	1651.57
<i>T</i> /K	293	173
Crystal system	triclinic	triclinic
Space group	<i>P</i> $\bar{1}$	<i>P</i> $\bar{1}$
<i>a</i> /Å	13.319(2)	12.847(1)
<i>b</i> /Å	17.472(2)	13.511(1)
<i>c</i> /Å	18.380(3)	19.107(1)
α /°	84.59(1)	84.58(1)
β /°	80.87(1)	86.19(1)
γ /°	86.56(1)	86.95(1)
<i>V</i> /Å ³	4199	3290.9
<i>Z</i>	2	2
ρ_{calc} /g cm ⁻³	1.436	1.667
μ (Mo-K α)/mm ⁻¹	3.893	4.498
Reflections collected	16179	15019
Independent reflections	9089 [<i>I</i> > 3 σ (<i>I</i>)]	11092 [<i>I</i> > 2 σ (<i>I</i>)]
Final <i>R</i> ₁	0.0506	0.0414
<i>R</i> _w	0.0485	0.1156

[Pt₂Cl(μ -H)(μ -PPh₂)(PPh₃)₃]PF₆ (8a**).** Complex **4** in a CH₂Cl₂ solution transformed into **8a** in 1 day at room temperature, the HCl originating from the solvent. Evaporation of the solvent to dryness afforded **8a** quantitatively. Its purity was monitored by $^{31}P\{^1H\}$ NMR in CH₂Cl₂/C₆D₆. See NMR details in Table 2.

[Pt₂Cl(μ -H)(μ -PPh₂)(PPh₃)₃]SO₃CF₃ (8b**).** Pure CF₃SO₃H (4.4 μ L, 0.05 mmol), then HCl (4.2 μ L, 37% in H₂O, 0.05 mmol) were added to a solution of **1** (68.0 mg, 0.05 mmol) in THF (10 mL). The colour of the solution rapidly changed from orange to red, and then to yellow. After the solution was stirred for 5 h at room temperature, the solvent was removed under reduced pressure and the product dried *in vacuo*. The spectroscopic yield ($^{31}P\{^1H\}$ NMR) was quantitative and the purity of **8b** was monitored by $^{31}P\{^1H\}$ NMR in a mixture of CH₂Cl₂ and C₆D₆. Details of the 1H and $^{31}P\{^1H\}$ NMR data are summarized in Table 2. FABMS (p - $O_2NC_6H_4CH_2OH$) (NBA matrix): m/z 1397.8 (M $^+$), 1134.8 (M - PPh₃) $^+$.

[Pt₂Br(μ -H)(μ -PPh₂)(PPh₃)₃]PF₆ (9**).** HPF₆ (10.5 μ L, 75% in H₂O, 0.1 mmol), then HBr (114 μ L, 48% in H₂O diluted 10 times, 0.1 mmol) were added to a solution of **1** (136.0 mg, 0.1 mmol) in THF (30 mL). The colour of the solution rapidly changed from orange to colourless. After the solution was stirred for 3 h at room temperature, the solvent was removed under reduced pressure and the purity of the solid was monitored by $^{31}P\{^1H\}$ NMR in CD₂Cl₂. Details of the 1H and $^{31}P\{^1H\}$ NMR data are summarized in Table 2.

Crystallographic studies

Experimental details are given in Table 4. Unit cell parameters for **2** were determined from 25 reflections having $2^\circ < 2\theta < 15^\circ$. The data were corrected for Lorentz and polarization effects and an empirical absorption correction was applied (DIFABS).⁴⁰ Data reduction was made by SDP package with decay correction.⁴¹ The position of the copper and platinum atoms was deduced from the Patterson map and subsequent sets of Fourier and difference Fourier synthesis in the *P* $\bar{1}$ space group revealed the entire structure.⁴² The fractional coordinates of all hydrogen atoms were calculated and these atoms were assigned constant isotropic temperature factors equal those of the bonded carbon. The PF₆⁻ anion has a high thermal agitation with two positions for each fluorine atom, so that the coordinates of these seven atoms were fixed at the observed positions in the map. Full least-squares refinement minimizing the function $\sum w(|F_o| - |F_c|)^2$ converged to the *R* values given in

Table 4. Atomic scattering factors and anomalous dispersion corrections were taken from standard sources.^{42,43}

For $6 \cdot 0.5\text{CH}_2\text{Cl}_2$, quantitative data were obtained at -100°C using a Nonius Kappa CCD diffractometer (see Table 4). The resulting data-set was transferred to a DEC Alpha workstation, and for all subsequent calculations the Nonius OpenMoleN package was used.⁴⁴ The structure was solved using direct methods. Absorption corrections are part of the scaling procedure of data reduction. After refinement of the heavy atoms, a difference-Fourier map revealed maximas of residual electronic density close to the positions expected for hydrogen atoms; they were introduced as fixed contributors in structure factor calculations by their computed coordinates ($\text{C-H} = 0.95 \text{ \AA}$) and isotropic temperature factors such as $B(\text{H}) = 1.3 B_{\text{eqv}}(\text{C}) \text{ \AA}^2$ but not refined; the hydride bridging between the Pt atoms and the CH_2Cl_2 protons were omitted. Full least-squares refinements on $|F^2|$. A final difference map revealed no significant maxima. The scattering factor coefficients and anomalous dispersion coefficients come respectively from ref. 45a and b.

CCDC reference numbers 189281 (2) and 188401 ($6 \cdot 0.5\text{CH}_2\text{Cl}_2$).

See <http://www.rsc.org/suppdata/dt/b2/b206347f/> for crystallographic data for 188401 in CIF or other electronic format.

Acknowledgements

We are grateful to Prof. J. Fischer and Dr. A. DeCian (Strasbourg) for the X-ray structure determination of $6 \cdot 0.5\text{CH}_2\text{Cl}_2$ and to Prof. R. Welter (Strasbourg) and Ms. F. Porcher (Nancy) for assistance. We thank the Centre National de la Recherche Scientifique and the Ministère de la Recherche for support. This project was also supported by the Fonds International de Coopération Universitaire – FICU (AUPELF-UREF, Agence Universitaire de la Francophonie).

References

- 1 G. K. Anderson, *Adv. Organomet. Chem.*, 1993, **35**, 1.
- 2 L. Mole, J. L. Spencer, S. A. Litster, A. D. Redhouse, N. Carr and A. G. Orpen, *J. Chem. Soc., Dalton Trans.*, 1996, 2315.
- 3 (a) P. Leoni, S. Manetti and M. Pasquali, *Inorg. Chem.*, 1995, **34**, 749; (b) P. Mastroilli, M. Palma, F. P. Fanizzi and C. F. Nobile, *J. Chem. Soc., Dalton Trans.*, 2000, 4272; (c) E. Alonso, J. Fornies, C. Fortuno, A. Martin and A. G. Orpen, *Organometallics*, 2001, **20**, 850.
- 4 A. L. Bandini, G. Banditelli and G. Minghetti, *J. Organomet. Chem.*, 2000, **595**, 224.
- 5 J. Chatt and J. M. Davidson, *J. Chem. Soc. A*, 1964, 2433.
- 6 E. A. V. Ebsworth, H. M. Ferrier, B. J. L. Henner, D. W. H. Rankin, F. J. S. Reed, H. E. Robertson and J. D. Whitelock, *Angew. Chem., Int. Ed. Engl.*, 1977, **16**, 482.
- 7 J. Jans, R. Naegeli, L. M. Venanzi and A. Albinati, *J. Organomet. Chem.*, 1983, **247**, C37.
- 8 A. R. Siedle, R. A. Newmark and W. B. Gleason, *J. Am. Chem. Soc.*, 1986, **108**, 767.
- 9 P. W. N. M. van Leeuwen, C. F. Roobeek, J. H. G. Frijns and A. G. Orpen, *Organometallics*, 1990, **9**, 1211.
- 10 P. Leoni, M. Pasquali, A. Fortunelli, G. Germano and A. Albinati, *J. Am. Chem. Soc.*, 1998, **120**, 9564.
- 11 M. Green, J. L. Spencer, F. G. A. Stone and C. A. Tsipis, *J. Chem. Soc., Dalton Trans.*, 1977, 1525.
- 12 C. A. Tsipis, *J. Organomet. Chem.*, 1980, **187**, 427.
- 13 R. Bender, S.-E. Bouaoud, P. Braunstein, Y. Dusausoy, N. Merabet, J. Raya and D. Rouag, *J. Chem. Soc., Dalton Trans.*, 1999, 735.
- 14 M. A. Bennett, D. E. Berry, S. K. Bhargava, E. J. Ditzel, G. B. Robertson and A. C. Willis, *J. Chem. Soc., Chem. Commun.*, 1987, 1613.
- 15 M. A. Bennett, D. E. Berry and K. A. Beveridge, *Inorg. Chem.*, 1990, **29**, 4148.
- 16 R. Bender, P. Braunstein, A. Dedieu and Y. Dusausoy, *Angew. Chem., Int. Ed. Engl.*, 1989, **28**, 923.
- 17 P. Leoni, M. Pasquali, M. Sommovigo, M. Laschi, P. Zanello, A. Albinati, F. Lianza, P. S. Pregosin and H. Rügger, *Organometallics*, 1993, **12**, 1702.
- 18 P. Leoni, G. Pieri and M. Pasquali, *J. Chem. Soc., Dalton Trans.*, 1998, 657.
- 19 T. Blum, P. Braunstein, A. Tiripicchio and M. Tiripicchio-Camellini, *New J. Chem.*, 1988, **12**, 539.
- 20 T. Blum and P. Braunstein, *Organometallics*, 1989, **8**, 2497.
- 21 (a) I. D. Salter, in *Comprehensive Organometallic Chemistry II*, ed. E. W. Abel, F. G. A. Stone and G. Wilkinson, Pergamon Press, Oxford, 1995; (b) T. Beringhelli, G. D'Alfonso, M. G. Garavaglia, M. Panigati, P. Mercandelli and A. Sironi, *Organometallics*, 2002, **21**, 2705 and references cited.
- 22 P. Braunstein, S. Freyburger and O. Bars, *J. Organomet. Chem.*, 1988, **352**, C29.
- 23 S. A. Batten, J. C. Jeffery, P. L. Jones, D. F. Mullica, M. D. Rudd, E. L. Sappenfield, F. G. A. Stone and A. Wolf, *Inorg. Chem.*, 1997, **36**, 2570.
- 24 T. Tanase, H. Toda and Y. Yamamoto, *Inorg. Chem.*, 1997, **36**, 1571.
- 25 J. C. Dyason, P. C. Healy, M. Engelhardt, C. Pakawatchai, V. A. Patrick, C. L. Raston and A. H. White, *J. Chem. Soc., Dalton Trans.*, 1985, 831.
- 26 P. E. Garrou, *Chem. Rev.*, 1985, **85**, 171.
- 27 C. Archambault, R. Bender, P. Braunstein, A. DeCian and J. Fischer, *Chem. Commun.*, 1996, 2729.
- 28 (a) W. Beck and K. Sünkel, *Chem. Rev.*, 1988, **88**, 1405; (b) G. A. Lawrance, *Chem. Rev.*, 1986, **86**, 17.
- 29 J. Fischer and A. DeCian, personal communication, 2000.
- 30 H. Bauer, U. Nagel and W. Beck, *J. Organomet. Chem.*, 1985, **290**, 219.
- 31 M. A. Bennett, T. W. Matheson, G. B. Robertson, W. L. Steffen and T. W. Turney, *J. Chem. Soc., Chem. Commun.*, 1979, 32.
- 32 K. Sünkel, G. Urban and W. Beck, *J. Organomet. Chem.*, 1985, **290**, 231.
- 33 R. Fernández-Galán, B. R. Manzano, A. Otero, M. Lanfranchi and M. A. Pellinghelli, *Inorg. Chem.*, 1994, **33**, 2309.
- 34 E. Horn and M. R. Snow, *Aust. J. Chem.*, 1980, **33**, 2369.
- 35 U. Bossek, G. Haselhorst, S. Ross, K. Wieghardt and B. Nuber, *J. Chem. Soc., Dalton Trans.*, 1994, 2041.
- 36 D. L. Reger, M. F. Huff and L. Lebioda, *Acta Crystallogr.*, 1991, **C47**, 1167.
- 37 E. Alonso, J. Fornies, C. Fortuno, A. Martin and A. G. Orpen, *J. Chem. Soc., Chem. Commun.*, 1996, 231.
- 38 D. Nobel, G. van Koten and A. L. Spek, *Angew. Chem., Int. Ed. Engl.*, 1989, **28**, 208.
- 39 G. van Koten, *J. Organomet. Chem.*, 1990, **400**, 283.
- 40 N. Walker and D. Stuart, *Acta Crystallogr.*, 1983, **A39**, 159.
- 41 SDP Structure Determination Package, Enraf-Nonius, Delft, 1977.
- 42 G. M. Sheldrick, *Programs for Crystal Structure Determination*; University of Göttingen, Göttingen, West Germany, 1976.
- 43 *International Tables for X-ray Crystallography*, Kynoch, Birmingham, England, 1974, vol. IV.
- 44 *OpenMoleN, Interactive Structure Solution*, Nonius B.V., Delft, The Netherlands, 1997.
- 45 D. T. Cromer and J. T. Waber, *International Tables for X-ray Crystallography*, 1974, vol. IV, The Kynoch Press, Birmingham, (a) Table 2.2b; (b) Table 2.3.1.